

This is the peer reviewed version of the following article:

Analytical bounds for the electromechanical buckling of a compressed nanocantilever / Radi, E.; Bianchi, G.; di Ruvo, L.. - In: APPLIED MATHEMATICAL MODELLING. - ISSN 0307-904X. - 59:(2018), pp. 571-582. [10.1016/j.apm.2018.02.007]

*Terms of use:*

The terms and conditions for the reuse of this version of the manuscript are specified in the publishing policy. For all terms of use and more information see the publisher's website.

06/07/2024 21:03

(Article begins on next page)

Dear author,

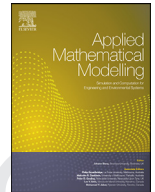
Please note that changes made in the online proofing system will be added to the article before publication but are not reflected in this PDF.

We also ask that this file not be used for submitting corrections.



Contents lists available at ScienceDirect

## Applied Mathematical Modelling

journal homepage: [www.elsevier.com/locate/apm](http://www.elsevier.com/locate/apm)

# Analytical bounds for the electromechanical buckling of a compressed nanocantilever

Q1 Enrico Radi\*, Giovanni Bianchi, Lorenzo di Ruvo

Dipartimento di Scienze e Metodi dell'Ingegneria, Università di Modena e Reggio Emilia, via G. Amendola 2, 42122 Reggio Emilia, Italy

## ARTICLE INFO

### Article history:

Received 29 August 2017

Revised 20 January 2018

Accepted 12 February 2018

Available online xxx

### Keywords:

Pull-in voltage

MEMS

Q2 NEMS

Nanocantilever

Casimir force

Van der Waals force

Buckling load

## ABSTRACT

An analytical approach is presented for the accurate definition of lower and upper bounds for the pull-in voltage and tip displacement of a micro- or nanocantilever beam subject to compressive axial load, electrostatic actuation and intermolecular surface forces. The problem is formulated as a nonlinear two-point boundary value problem and has been transformed into an equivalent nonlinear integral equation. Initially, new analytical estimates are found for the beam deflection, which are then employed for assessing novel and accurate bounds from both sides for the pull-in parameters, taking into account for the effects of the compressive axial load. The analytical predictions are found to closely agree with the numerical results provided by the shooting method. The effects of surface elasticity and residual stresses, which are of significant importance when the physical dimensions of structures descend to nanosize, can also be included in the proposed approach.

© 2018 Published by Elsevier Inc.

## 1. Introduction

Q3 Several MEMS and NEMS current applications in sensors, actuators and memory devices [1,2] exploit the switching between two stable positions of a flexible electrode nanobeam suspended above a fixed electrode. Under the action of the electrostatic force the nanocantilever deflects toward to the ground and the electrostatic force increases correspondingly. At the pull-in voltage the micro-beam leaves the principal equilibrium path, which becomes unstable, and pulls-in onto the fixed electrode, thus creating an electrical connection. Since the pull-in voltage determines operation voltage and power dissipation, its accurate determination becomes of the primary importance in MEMS and NEMS design. On one side, a low pull-in voltage implies a limited power consumption and small amount of energy stored in the system, thus enhancing the device performance [1]. A method for reducing the pull-in voltage consists in applying a compressive axial load to the nanobeam. On the other side, if the pull-in voltage is too small, the intermolecular surface forces may cause the collapse of the nanocantilever tip onto the fixed electrode, even in the absence of electrostatic actuation. These quantum mechanical interactions are usually described by van der Waals (vdW) or Casimir forces according to the gap between the electrodes [3]. Their effects are negligible for MEMS, where the separation distance is of the order of micron, but they play a significant role for NEMS, where the gap descends to the nanoscale.

The cantilever beam deflection is described by a nonlinear fourth-order boundary value problem (BVP) that can be solved by using approximate approaches only. The most exploited ones are based on the assumption of 1D lumped models or specific shape functions for the beam deflection. Perturbation approaches or Taylor series expansions of the loading term

\* Corresponding author.

E-mail addresses: [eradi@unimore.it](mailto:eradi@unimore.it), [eradi@libero.it](mailto:eradi@libero.it) (E. Radi).

18 have been frequently employed also. Detailed information can be found in review papers by Lin and Zhao [4], Chuang et  
19 al. [5], Zhang et al. [6]. However, these approximated methods provide random estimates of the pull-in parameters and  
20 their accuracy considerably decreases as the actuation voltage gets closer to the pull-in voltage. In order to be effective, the  
21 approach should instead offer accurate lower and upper bounds, both for the pull-in voltage and tip deflection.

22 According to the theory of elastic stability, slender beams have critical compressive load limits beyond which they buckle  
23 [7]. If they are also subject to electrostatic loading, their deflection increases nonlinearly with the magnitude of the com-  
24 pressive axial load. Therefore, the determination of the electromechanical buckling (EMB) characteristics of axially-loaded  
25 nanobeams is essential for designing such devices [8–12]. Indeed, the application of an adaptable compressive load, e.g. by  
26 means of an axial elastic constraint applied at the tip of the beam, allows to modify the deflection and the pull-in behavior  
27 of a nanocantilever. It may also affect the occurring of stiction [13–15], namely the phenomenon that takes place when the  
28 intermolecular surface forces overcome the restoring elastic forces and keep the cantilever tip attached to the ground. In  
29 general, stiction may be avoided or favoured by reducing or increasing the axial compressive load, respectively. Stiction has  
30 been advantageously exploited in applications such as non-volatile memory cells, since it allows holding the switch in the  
31 closed state with no need for supplying continued power input. On the contrary, in sensor and actuator applications it may  
32 cause permanent adhesion and other unexpected occurrences that may reduce the range of operability of the device.

33 The axial load provides an additional linear second-order term in the governing fourth-order ODE of the Eulero-Bernoulli  
34 (EB) beam model, which can either stiffen, if tensile, or soften, if compressive, the nanostructure. Many authors investigated  
35 the influence of the axial load and, in general, of the additional second-order term on the beam pull-in displacement and  
36 voltage by using a numerical approach [3,16–20]. They clearly found that critical pull-in voltage decreases under the action  
37 of a compressive axial load, whereas an opposite stiffening effect is observed for a tensile axial load. Therefore, the presence  
38 of a compressive axial load is an important issue in the fabrication and design of sensors and actuators, because it may  
39 cause degradation or even failure of the devices.

40 The work [21] focuses on the effects of the support flexibility on the pull-in instability of an electrostatically actuated  
41 micro- or nanocantilever and accurate analytical bounds are found for the pull-in parameter in the absence of axial load.  
42 The present work focuses instead on the effects of a compressive axial load on the pull-in instability. To this aim, the  
43 analytical approach proposed in [21] is extended by taking into consideration an additional term in the governing ODE  
44 and in the boundary conditions coming from the contribution of the axial load. This contribution is indeed expected to  
45 have a significant influence on the pull-in parameters [3,22] as well as on the critical gap for a freestanding compressed  
46 nanocantilever, which is an essential parameter in the design of NEMS for avoiding the collapse of the flexible electrode  
47 on the ground plane when the electrostatic loading is removed. Moreover, the additional term may also include the effects  
48 of surface elasticity and residual stresses, which are important factors that may explain the experimentally measured size  
49 dependent behavior of nanobeams.

50 The nonlinear BVP governing the beam deflection is presented in Section 2 and then transformed into an equivalent  
51 nonlinear integral equation by using the Green's function of the compressed cantilever beam. Here, we consider a linear  
52 elastic EB beam subject to a distributed load that depends nonlinearly on the beam deflection. The total deflection of the  
53 beam is formally given by the sum of all the contributions offered by the load acting on each infinitesimal part of the beam.  
54 Therefore, it can be calculated by exploiting the Green's function of the compressed cantilever EB beam. A similar approach  
55 has been employed also in the papers [3,21], where the contribution of the axial load has not been introduced. The solution  
56 of the extended BVP considered here is then proved to be positive, monotonic and convex and novel lower and upper  
57 estimates on the deflection are obtained in Section 3. These estimates are then employed in Section 4 for assessing novel  
58 and accurate bounds from both sides for the pull-in in voltage and tip deflection, taking into account for the effects of the  
59 compressive axial load. Estimates of the critical level of the intermolecular surface forces causing the pull-in instability in the  
60 absence of electrostatic loading are also provided for various values of the axial compressive load. The proposed approach is  
61 then validated in Section 5 by comparing the analytical estimates with the numerical solution of the BVP obtained by using  
62 the shooting method.

63 Since no closed form solution can be achieved for the extremely nonlinear BVP governing the pull-in instability of a  
64 micro- or nanobeam subject to a compressive axial force, but, to authors' knowledge, only numerical or approximate meth-  
65 ods have been proposed in the Literature – e.g. differential quadrature method, Adomian decomposition method, finite el-  
66 ement method and the Galerkin method - then, the analytical bounds provided here can be considered as extremely useful  
67 for validating the number of numerical strategies and approximated methods used for approaching this very difficult non-  
68 linear BVP. Moreover, the approach is flexible enough to allow for further generalization aiming to consider more complex  
69 interactions arising at the micro- and nanoscale, such as electrochemical and double layer interactions.

## 70 2. Mathematical model

71 The problem of an elastic micro- or nanocantilever clamped at one end and subject to electrostatic actuation with the  
72 effects of fringing field, vdW or Casimir forces, and compressive axial load  $P$ , sketched in Fig. 1, can be described by the  
73 following fourth-order, non-linear ODE

$$u^{IV}(x) + k^2 u''(x) = f(u(x)), \quad \text{for } x \in [0, 1], \quad (1)$$

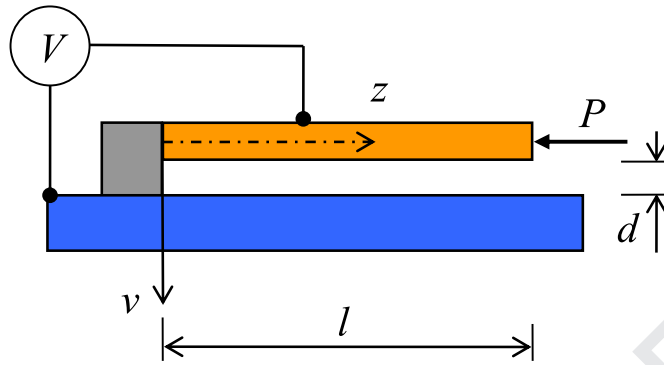


Fig. 1. A compressed micro/nanocantilever under electrostatic actuation.

74 where  $u = v/d$  and  $x = z/l$  are nondimensional variables, being  $v$  the beam deflection,  $d$  the initial gap between the electrodes,  
 75  $z$  the position along the beam as measured from the clamped end, and  $l$  the beam length, so that  $0 \leq z \leq l$ , and the apex de-  
 76 notes differentiation with respect to  $x$ . The loading term in (1) includes the contributions of electrostatic actuation, fringing  
 77 field and van der Waals or Casimir forces, namely

$$f(u) = \frac{\gamma \beta}{1-u} + \frac{\beta}{(1-u)^2} + \frac{\alpha_w}{(1-u)^3} + \frac{\alpha_c}{(1-u)^4}, \tag{2}$$

78 being  $\gamma = 0.65 d/w$  the fringing coefficient, where  $w$  is the cross-section width. The nondimensional parameters  $\beta$ ,  $\alpha_w$  and  
 79  $\alpha_c$  are given by

$$\beta = \frac{\epsilon_0 w V^2 l^4}{2 d^3 E I}, \quad \alpha_w = \frac{A w l^4}{6 \pi d^4 E I}, \quad \alpha_c = \frac{\pi^2 h c w l^4}{240 d^5 E I}, \tag{3}$$

80 where  $V$  is the electric voltage applied to the electrodes,  $E$  is the Young's modulus of the elastic material and  $I$  is the moment  
 81 of inertia of the beam cross-section,  $\epsilon_0 = 8.854 \times 10^{-12} C^2 N^{-1} m^{-2}$  is the permittivity of vacuum,  $A$  is the Hamaker constant,  
 82  $h = 1.055 \times 10^{-34} Js$  is the Planck's constant divided by  $2\pi$ ,  $c = 2.998 \times 10^8 m/s$  is the speed of light.

83 The boundary conditions for the cantilever beam then require vanishing of displacement and rotation of the cross section  
 84 at  $x=0$ , and vanishing of the bending moment and shearing force at  $x=1$ , namely [7]

$$u(0) = 0, \quad u'(0) = 0, \quad u''(1) = 0, \quad u'''(1) + k^2 u'(1) = 0, \tag{4}$$

85 where the non-dimensional parameter

$$k = \sqrt{\frac{P l^2}{E I}}, \tag{5}$$

86 denotes the square root of the ratio between the compressive axial load  $P$  and the beam bending stiffness. The buckling  
 87 axial load for a cantilever EB beam is attained as  $k$  approaches  $\pi/2$  [7]. Therefore, in the following we assume  $0 \leq k < \pi/2$ .

88 Since the scale effect of the nanostructure is generally compatible with the size of molecular and/or atomic interactions,  
 89 advanced beam models are usually required for an accurate simulation, such as those derived by the non-local or couple  
 90 stress elastic theory [10,11,19,20,23]. These sophisticated constitutive models contain an internal length scale as a material  
 91 parameter, which introduce in the governing ODE (1) a further term proportional to the second derivative. The effects of  
 92 surface tension and residual stresses are also significant in nanobeams. They occur because the physical properties of surface  
 93 layer are different from that of the bulk of nanoscale material and structure. For conductive metals these effects appear at  
 94 the submicron scale. They have been simulated in many recent works by using enhanced constitutive models accounting for  
 95 surface elasticity [24–27].

96 All these contributions can be included in the present model just by modifying the value of the parameter  $k$  and/or  
 97 introducing additional terms in the flexural stiffness  $EI$  of the nanobeam [28–32].

98 **2.1. Nonlinear integral equation formulation**

99 The nonlinear BVP (1) and (4) can be equivalently formulated by means of a nonlinear integral equation once the Green's  
 100 function  $G(t)$  of the differential problem is worked out, as done in [21] for a nanocantilever in the absence of the axial load.  
 101 The deflection of a cantilever EB beam subject to a compressive axial load and a transversal unit load acting at position  $x$  is  
 102 described by the following linear ODE

$$G^{IV}(t) + k^2 G''(t) = \delta(x-t). \tag{6}$$

103 where  $\delta(x)$  denotes the Dirac delta function. The general solution to the ODE (6) is

$$104 \quad G(t) = \begin{cases} A_0 + A_1 t + A_2 \cos kt + A_3 \sin kt, & 0 \leq t < x, \\ B_0 + B_1 t + B_2 \cos kt + B_3 \sin kt, & x < t \leq 1. \end{cases} \quad (7)$$

The eight constants  $A_i$  and  $B_i$  ( $i=0,1,2,3$ ) can be determined by using the boundary conditions (4), namely

$$105 \quad G(0)=0, \quad G'(0) = 0, \quad G''(1) = 0, \quad G'''(1) + k^2 G'(1) = 0, \quad (8)$$

and the continuity conditions at  $t=x$  for the deflection, slope, bending moment and shear force

$$106 \quad G(x^+) = G(x^-), \quad G'(x^+) = G'(x^-), \quad G''(x^+) = G''(x^-), \quad (9)$$

$$G'''(x^+) + k^2 G'(x^+) - G'''(x^-) - k^2 G'(x^-) = 1,$$

respectively, thus providing

$$107 \quad G(t) \begin{cases} \{\sin kt - kt + (1 - \cos kt)[\sin kx + (1 - \cos kx) \tan k]/k^3, & 0 \leq t < x, \\ \{\sin kx - kx + (1 - \cos kx)[\sin kt + (1 - \cos kt) \tan k]/k^3, & x < t \leq 1. \end{cases} \quad (10)$$

Therefore, the BVP (1) and (4) is equivalent to the following non-linear integral equation

$$108 \quad u(x) = \frac{1}{k^3} \int_0^x \{\sin kt - kt + (1 - \cos kt)[\sin kx + (1 - \cos kx) \tan k]\} f(u(t)) dt \\ + \frac{1}{k^3} \int_x^1 \{\sin kx - kx + (1 - \cos kx)[\sin kt + (1 - \cos kt) \tan k]\} f(u(t)) dt. \quad (11)$$

As  $k \rightarrow 0$ , the non-linear integral Eq. (11) recovers that obtained in [3,33,34] for a cantilever EB beam not axially loaded.

109 According to (11), the normalized deflection of the cantilever tip then is given by

$$110 \quad u(1) = \frac{1}{k^3} \int_0^1 [\sin kt - kt + (1 - \cos kt) \tan k] f(u(t)) dt. \quad (12)$$

By taking the derivatives of Eq. (11) one obtains

$$111 \quad u'(x) = \frac{\cos kx + \sin kx \tan k}{k^2} \int_0^x (1 - \cos kt) f(u(t)) dt \\ + \frac{1}{k^2} \int_x^1 \{[\sin kt + (1 - \cos kt) \tan k] \sin kx + \cos kx - 1\} f(u(t)) dt, \quad (13)$$

$$112 \quad u''(x) = \frac{\cos kx \tan k - \sin kx}{k} \int_0^x (1 - \cos kt) f(u(t)) dt \\ + \frac{1}{k} \int_x^1 \{[\sin kt + (1 - \cos kt) \tan k] \cos kx - \sin kx\} f(u(t)) dt, \quad (14)$$

$$113 \quad u'''(x) = -(\cos kx + \sin kx \tan k) \int_0^x (1 - \cos kt) f(u(t)) dt \\ - \int_x^1 \{[\sin kt + (1 - \cos kt) \tan k] \sin kx + \cos kx\} f(u(t)) dt, \quad (15)$$

and, thus, the following lemma holds true.

114 **Lemma 2.1.** Let  $u(x)$  be the solution to the nonlinear integral Eq. (11), then the following conditions hold for  $f(u) \geq 0$ ,  $k \in [0$ ,  
115  $\pi/2)$  and  $x \in [0, 1]$ :

$$116 \quad u(x) \geq 0, \quad u'(x) \geq 0, \quad u''(x) \geq 0, \quad u'''(x) \leq 0. \quad (16)$$

**Proof.** Conditions (16) follow from Eqs. (11), (13)–(15), respectively, being

$$117 \quad [\sin kt + (1 - \cos kt) \tan k] \sin kx + \cos kx \\ \geq [\sin kx + (1 - \cos kx) \tan kx] \sin kx + \cos kx = \frac{1}{\cos kx} \geq 1, \quad (17)$$

$$118 \quad [\sin kt + (1 - \cos kt) \tan k] \cos kx - \sin kx \\ \geq [\sin kt + (1 - \cos kt) \tan k] \cos kx - \sin kx = (\tan kt - \tan kx) \cos kx \geq 0, \quad (18)$$

for  $t \in [x, 1]$ .

119 Therefore, the function  $u$  is positive, increasing and convex for compressive axial load.

### 120 3. A priori estimates on the beam deflection

121 We prove here some bounds for the solution of the BVP (1) and (11) for  $0 \leq u(x) \leq 1$ .

122 Let us start by providing an upper bound for the solution  $u(x)$  to the problem (1) and (4).

123 **Lemma 3.1.** Let  $u(x)$  be the solution to the BVP (1) and (4), then

$$124 \quad u(x) \leq u(1)b(x), \quad \text{for } x \in [0, 1], \quad (19)$$

124 where

$$b(x) = \frac{1}{3} \left[ 6x^2 - 4x^3 + x^4 - \frac{4k^2}{18 - k^2} (3x^2 - 5x^3 + 2x^4) \right]. \quad (20)$$

125 **Proof.** Let us introduce the function

$$h(x) = u(1) \left( 2x^2 - \frac{4}{3}x^3 + \frac{1}{3}x^4 \right) - \frac{k^2}{3} u'(1) \left( \frac{1}{2}x^2 - \frac{5}{6}x^3 + \frac{1}{3}x^4 \right) - u(x), \quad (21)$$

126 whose derivatives are

$$h'(x) = 4u(1) \left( x - x^2 + \frac{1}{3}x^3 \right) - \frac{k^2}{3} u'(1) \left( x - \frac{5}{2}x^2 + \frac{4}{3}x^3 \right) - u'(x),$$

$$h''(x) = 4u(1) (1 - 2x + x^2) - \frac{k^2}{3} u'(1) (1 - 5x + 4x^2) - u''(x),$$

$$h'''(x) = -8u(1) (1 - x) + \frac{k^2}{3} u'(1) (5 - 8x) - u'''(x),$$

$$h^{IV}(x) = 8 \left[ u(1) - \frac{k^2}{3} u'(1) \right] - u^{IV}(x),$$

$$h^V(x) = -u^V(x) = -\frac{df(u)}{du} u'(x) + k^2 u'''(x) \leq 0. \quad (22)$$

127 The latter inequality follows from (16), (1) and (2) for  $u(x) \leq 1$ , being

$$\frac{df(u)}{du} = \frac{\gamma \beta}{(1-u)^2} + \frac{2\beta}{(1-u)^3} + \frac{3\alpha_w}{(1-u)^4} + \frac{4\alpha_c}{(1-u)^5} \geq 0. \quad (23)$$

128 Therefore, the function  $h(x)$  satisfies the following conditions

$$h(0) = 0, \quad h(1) = 0, \quad h'(0) = 0, \quad h''(1) = 0, \quad h'''(1) = 0. \quad (24)$$

129 By using the mean value theorem, continuity of the function  $h(x)$  and conditions (24)<sub>1,2</sub> imply that there exists  $x_1 \in [0,$   
 130  $1]$  such that  $h'(x_1) = 0$ . Then, by using conditions (24)<sub>3,4</sub> there exists  $x_2 \in [0, x_1]$  such that  $h''(x_2) = 0$  and also  $x_3 \in [x_2, 1]$   
 131 such that  $h'''(x_3) = 0$ . Moreover,  $h'''(x)$  is concave being  $h^V(x) \leq 0$ . It follows that  $h''(x) \leq 0$  for  $x \in [x_2, 1]$  and  $h''(x) \geq 0$  for  $x$   
 132  $\in [0, x_2]$ , and thus  $h'(x) \geq 0$  for  $x \in [0, x_1]$  and  $h'(x) \leq 0$  for  $x \in [x_1, 1]$ . Since  $h(0) = h(1) = 0$ , then it necessarily follows that  
 133  $h(x) \geq 0$  for  $x \in [0, 1]$ , namely

$$u(x) \leq u(1) \left( 2x^2 - \frac{4}{3}x^3 + \frac{1}{3}x^4 \right) - \frac{k^2}{3} u'(1) \left( \frac{1}{2}x^2 - \frac{5}{6}x^3 + \frac{1}{3}x^4 \right), \quad \text{for } x \in [0, 1] \quad (25)$$

134 Moreover, from the conditions  $h'(1) \leq 0$  and  $h''(0) \geq 0$ , by using (22) one obtains

$$h'(1) = \frac{4}{3} u(1) - \left( 1 - \frac{k^2}{18} \right) u'(1) \leq 0, \quad h''(0) = 4u(1) - \frac{k^2}{3} u'(1) - u''(0) \geq 0, \quad (26)$$

135 and thus

$$u'(1) \geq \frac{24}{18 - k^2} u(1), \quad u''(0) \leq 4u(1) - \frac{k^2}{3} u'(1) \leq 12 \frac{6 - k^2}{18 - k^2} u(1). \quad (27)$$

136 The introduction of (27)<sub>1</sub> in the inequality (25), considering that the term multiplying  $u'(1)$  is non negative for  $x \in [0,$   
 137  $1]$ , then yields the upper bound (19).

138 From conditions (16)<sub>4</sub> and (27)<sub>2</sub> it follows that

$$u''(x) \leq u''(0) \leq 12 \frac{6 - k^2}{18 - k^2} u(1), \quad (28)$$

139 and thus from (1) and (28) one obtains the following lower bound for  $u^{IV}$

$$u^{IV}(x) \geq \beta^* - 12k^2 \frac{6 - k^2}{18 - k^2} u(1), \quad (29)$$

140 being  $f(u) \geq \beta^*$ , where

$$\beta^* = \beta(1 + \gamma) + \alpha_w + \alpha_c. \quad (30)$$

141 The result (19) holds also in the absence of the compressive axial load, namely for  $k=0$ , as stated in the next corollary  
142 that follows from Lemma 3.1.

143 **Corollary 3.1.** Let  $u_0(x)$  be the solution to the BVP (1) and (4) for  $k=0$  then

$$u_0(x) \leq u(1) \left( 2x^2 - \frac{4}{3}x^3 + \frac{1}{3}x^4 \right). \quad (31)$$

144 The same result was obtained in [35] and it has been recovered recently in [21] as a special case for an elastically  
145 constrained cantilever under electrostatic actuation.

146 In the following we derive a lower bound for the solution  $u(x)$  to the BVP (1) and (4).

147 **Lemma 3.2.** Let  $u(x)$  be the solution to the BVP (1) and (4), then

$$u(x) \geq u(1)a_1(x) + \beta^*a_2(x) \quad \text{for } x \in [0, 1], \quad (32)$$

148 where

$$a_1(x) = \frac{1}{2}(3x^2 - x^3) - \frac{k^2(6 - k^2)}{4(18 - k^2)}(3x^2 - 5x^3 + 2x^4), \quad a_2(x) = \frac{1}{48}(3x^2 - 5x^3 + 2x^4), \quad (33)$$

149 **Proof.** Let us introduce the following function

$$g(x) = u(x) - \frac{u(1)}{2} - (3x^2 - x^3) - \left[ \frac{\beta^*}{48} - \frac{k^2(6 - k^2)}{4(18 - k^2)} u(1) \right] (3x^2 - 5x^3 + 2x^4), \quad (34)$$

150 whose derivatives are

$$\begin{aligned} g'(x) &= u'(x) - \frac{3}{2}u(1)(2x - x^2) - \left[ \frac{\beta^*}{48} - \frac{k^2(6 - k^2)}{4(18 - k^2)} u(1) \right] (6x - 15x^2 + 8x^3), \\ g''(x) &= u''(x) - 3u(1)(1 - x) - \left[ \frac{\beta^*}{8} - \frac{3k^2(6 - k^2)}{2(18 - k^2)} u(1) \right] (1 - 5x + 4x^2), \\ g'''(x) &= u'''(x) + 3u(1) + \left[ \frac{\beta^*}{8} - \frac{3k^2(6 - k^2)}{2(18 - k^2)} u(1) \right] (5 - 8x), \\ g^{IV}(x) &= u^{IV}(x) - \beta^* + 12k^2 \frac{6 - k^2}{18 - k^2} u(1) \geq 0, \end{aligned} \quad (35)$$

151 where the latter inequality follows from relation (29). Therefore, the function  $g(x)$  satisfies the following conditions

$$g(0) = 0, \quad g(1) = 0, \quad g'(0) = 0, \quad g'(1) = 0. \quad (36)$$

152 By using the mean value theorem, continuity of  $g(x)$  together with conditions (36)<sub>1,2</sub> imply that there exists  $x_1 \in [0, 1]$   
153 such that  $g'(x_1) = 0$ . Moreover, by using conditions (36)<sub>3,4</sub> there exists  $x_2 \in [0, x_1]$  such that  $g''(x_2) = 0$  and also  $x_3 \in [x_2, 1]$   
154 such that  $g'''(x_3) = 0$ . Condition (35)<sub>4</sub> implies that  $g''(x)$  is convex. It follows that  $g''(x) \leq 0$  for  $x \in [x_2, 1]$  and  $g''(x) \geq 0$  for  $x$   
155  $\in [0, x_2]$ , and thus  $g'(x) \geq 0$  for  $x \in [0, x_1]$  and  $g'(x) \leq 0$  for  $x \in [x_1, 1]$ . Since  $g(0) = g(1) = 0$ , then it necessarily follows that  
156  $g(x) \geq 0$  for  $x \in [0, 1]$ , namely

$$u(x) \geq \frac{u(1)}{2} (3x^2 - x^3) + \left[ \frac{\beta^*}{48} - \frac{k^2(6 - k^2)}{4(18 - k^2)} u(1) \right] (3x^2 - 5x^3 + 2x^4), \quad \text{for } x \in [0, 1] \quad (37)$$

157 so that the lower bound (32) is attained.

158 The result (32) holds also in the absence of the compressive axial load, namely for  $k=0$ , as stated in the next corollary,  
159 which follows straight from Lemma 3.2.

160 **Corollary 3.2.** Let  $u_0(x)$  be the solution to the BVP (1) and (4) for  $k=0$ , then

$$u_0(x) \geq \frac{u(1)}{2} (3x^2 - x^3) + \frac{\beta^*}{48} (3x^2 - 5x^3 + 2x^4). \quad (38)$$

#### 161 4. Lower and upper bounds on the pull-in parameters

162 In the following we denote with  $r = u(1)$  the normalized deflection of the cantilever tip. By using (12) and the estimates  
163 (19), (32) and (27)<sub>1</sub> on the solution of the BVP (1) and (4), the following lower and upper bounds can be derived for the  
164 pull-in parameters  $\beta_{PI}$  and  $r_{PI}$ .



## 165 4.1. Lower bounds on the pull-in parameters

166 By using (19) and (20), from (12) it follows

$$\beta \geq \frac{rk^3 - F(r)}{L(r)}, \quad (39)$$

167 where the following functions can be calculated numerically

$$\begin{aligned} L(r) &= \int_0^1 \frac{\sin kt - kt + (1 - \cos kt) \tan k}{1 - rb(t)} \left( \gamma + \frac{1}{1 - rb(t)} \right) dt, \\ F(r) &= \int_0^1 \frac{\sin kt - kt + (1 - \cos kt) \tan k}{[1 - rb(t)]^3} \left( \alpha_W + \frac{\alpha_C}{1 - rb(t)} \right) dt. \end{aligned} \quad (40)$$

168 Inequality (39) defines a lower bound to the exact relation between the normalized voltage  $\beta$  and the normalized tip  
 169 deflection  $r$  provided by the solution of the BVP (1) and (4). Therefore, the maximum value of the left hand side of (39)  
 170 yields the lower bounds  $\beta_l$  and  $r_l$  for the pull-in parameters, such that  $\beta_{pl} \geq \beta_l$  and  $r_{pl} \geq r_l$ . Therefore, the lower bounds for  
 171 the pull-in parameters are given by the following equations obtained from the stationary condition of the left hand side of  
 172 (39)

$$\beta_l L(r_l) + F(r_l) = r_l k^3, \quad \beta_l L'(r_l) + F'(r_l) = k^3, \quad (41)$$

173 where also the following functions can be calculated numerically

$$\begin{aligned} L'(r) &= \int_0^1 \frac{\sin kt - kt + (1 - \cos kt) \tan k}{[1 - rb(t)]^2} \left( \gamma + \frac{2}{1 - rb(t)} \right) b(t) dt, \\ F'(r) &= \int_0^1 \frac{\sin kt - kt + (1 - \cos kt) \tan k}{[1 - rb(t)]^4} \left( 3\alpha_W + \frac{4\alpha_C}{1 - rb(t)} \right) b(t) dt. \end{aligned} \quad (42)$$

## 174 4.2. Upper bounds on the pull-in parameters

175 By using (32) and (33), from (12) it follows

$$r \geq [\beta K(r, \beta) + H(r, \beta)]/k^3, \quad (43)$$

176 where

$$\begin{aligned} K(r, \beta) &= \int_0^1 \frac{\sin kt - kt + (1 - \cos kt) \tan k}{1 - ra_1(t) - \beta^* a_2(t)} \left( \gamma + \frac{1}{1 - ra_1(t) - \beta^* a_2(t)} \right) dt, \\ H(r, \beta) &= \int_0^1 \frac{\sin kt - kt + (1 - \cos kt) \tan k}{[1 - ra_1(t) - \beta^* a_2(t)]^3} \left( \alpha_W + \frac{\alpha_C}{1 - ra_1(t) - \beta^* a_2(t)} \right) dt, \end{aligned} \quad (44)$$

177 where the parameter  $\beta^*$  has been defined in (30).

178 The inequality (43) defines an upper bound to the exact relation between the parameters  $\beta$  and  $r$ . Indeed, by equating  
 179 both sides of condition (43) we obtain an implicit relation for  $\beta$  as a function of  $r$  that is greater than the exact relation  
 180 provided by the solution of the BVP (1) and (4). The maximum value of the implicit function  $\beta(r)$  obtained from (43) by  
 181 using the stationary condition

$$\frac{d\beta}{dr} = 0, \quad (45)$$

182 then yields the upper bounds  $\beta_u$  and  $r_u$  for the pull-in parameters, such that  $\beta_{pl} \leq \beta_u$  and  $r_{pl} \leq r_u$ . Therefore, the upper  
 183 bounds for the pull-in parameters are given by the following conditions

$$\beta_u K(r_u, \beta_u) + H(r_u, \beta_u) = k^3 r_u, \quad \beta_u K'(r_u, \beta_u) + H'(r_u, \beta_u) = k^3, \quad (46)$$

184 where

$$\begin{aligned} K'(r, \beta) &= \int_0^1 \frac{\sin kt - kt + (1 - \cos kt) \tan k}{[1 - ra_1(t) - \beta^* a_2(t)]^2} \left( \gamma + \frac{2}{1 - ra_1(t) - \beta^* a_2(t)} \right) a_1(t) dt, \\ H'(r, \beta) &= \int_0^1 \frac{\sin kt - kt + (1 - \cos kt) \tan k}{[1 - ra_1(t) - \beta^* a_2(t)]^4} \left( 3\alpha_W + \frac{4\alpha_C}{1 - ra_1(t) - \beta^* a_2(t)} \right) a_1(t) dt. \end{aligned} \quad (47)$$

**Table 1**

Lower and upper bounds for the pull-in parameters of a micro/nanocantilever subjected to a compressive axial load with  $k=0.5$ , for several values of the vdW and Casimir parameters  $\alpha_W$ ,  $\alpha_C$ , and geometric ratio  $d/w$ .

$k=0.5$		$d/w=0$				$d/w=1$				$d/w=2$			
$\alpha_W$	$\alpha_C$	$r_l$	$\beta_l$	$r_u$	$\beta_u$	$r_l$	$\beta_l$	$r_u$	$\beta_u$	$r_l$	$\beta_l$	$r_u$	$\beta_u$
0.0	0.0	0.4433	1.5112	0.4520	1.5374	0.4873	1.0564	0.4960	1.0736	0.5139	0.8181	0.5226	0.8309
0.0	0.2	0.3771	1.0939	0.3853	1.1194	0.3978	0.7437	0.4060	0.7602	0.4086	0.5650	0.4168	0.5772
0.0	0.4	0.3347	0.7260	0.3428	0.7513	0.3461	0.4858	0.3543	0.5022	0.3518	0.3655	0.3601	0.3777
0.0	0.6	0.3022	0.3869	0.3103	0.4121	0.3075	0.2559	0.3159	0.2723	0.3102	0.1913	0.3186	0.2035
0.0	0.8	0.2753	0.0679	0.2835	0.0930	0.2762	0.0445	0.2846	0.0609	0.2766	0.0331	0.2852	0.0453
0.0	1.0	0.2522	-0.236	0.2604	-0.211	0.2494	-0.153	0.2580	-0.137	0.2481	-0.114	0.2568	-0.101
0.0	0.0	0.4433	1.5112	0.4520	1.5374	0.4873	1.0564	0.4960	1.0736	0.5139	0.8181	0.5226	0.8309
0.2	0.0	0.4168	1.2164	0.4255	1.2426	0.4468	0.8400	0.4556	0.8572	0.4635	0.6445	0.4723	0.6573
0.4	0.0	0.3945	0.9303	0.4032	0.9567	0.4150	0.6363	0.4238	0.6537	0.4259	0.4849	0.4348	0.4979
0.6	0.0	0.3751	0.6513	0.3838	0.6777	0.3882	0.4419	0.3971	0.4594	0.3950	0.3350	0.4041	0.3481
0.8	0.0	0.3577	0.3781	0.3664	0.4046	0.3648	0.2547	0.3738	0.2724	0.3684	0.1923	0.3776	0.2055
1.0	0.0	0.3419	0.1098	0.3507	0.1364	0.3438	0.0735	0.3530	0.0913	0.3448	0.0553	0.3542	0.0686

**Table 2**

Lower and upper bounds for the pull-in parameters of a micro/nanocantilever subjected to a compressive axial load with  $k=1$ , for several values of the vdW and Casimir parameters  $\alpha_W$ ,  $\alpha_C$ , and geometric ratio  $d/w$ .

$k=1$		$d/w=0$				$d/w=1$				$d/w=2$			
$\alpha_W$	$\alpha_C$	$r_l$	$\beta_l$	$r_u$	$\beta_u$	$r_l$	$\beta_l$	$r_u$	$\beta_u$	$r_l$	$\beta_l$	$r_u$	$\beta_u$
0.0	0.0	0.4460	1.0217	0.4545	1.0424	0.4901	0.7141	0.4987	0.7278	0.5167	0.5529	0.5255	0.5632
0.0	0.2	0.3573	0.6174	0.3654	0.6375	0.3728	0.4161	0.3812	0.4293	0.3808	0.3145	0.3892	0.3243
0.0	0.4	0.3054	0.2711	0.3135	0.2907	0.3109	0.1793	0.3194	0.1922	0.3137	0.1341	0.3223	0.1437
0.0	0.6	0.2666	-0.045	0.2748	-0.025	0.2658	-0.029	0.2744	-0.017	0.2654	-0.022	0.2742	-0.012
0.0	0.8	0.2351	-0.340	0.2433	-0.321	0.2294	-0.220	0.2381	-0.207	0.2267	-0.162	0.2356	-0.153
0.0	1.0	0.2082	-0.620	0.2165	-0.601	0.1986	-0.397	0.2073	-0.385	0.1940	-0.292	0.2030	-0.283
0.0	0.0	0.4460	1.0217	0.4545	1.0424	0.4901	0.7141	0.4987	0.7278	0.5167	0.5529	0.5255	0.5632
0.2	0.0	0.4082	0.7291	0.4168	0.7499	0.4333	0.5009	0.4421	0.5148	0.4470	0.3830	0.4559	0.3933
0.4	0.0	0.3782	0.4482	0.3868	0.4690	0.3916	0.3041	0.4006	0.3180	0.3986	0.2306	0.4078	0.2410
0.6	0.0	0.3528	0.1761	0.3616	0.1969	0.3576	0.1183	0.3668	0.1323	0.3600	0.0891	0.3694	0.0995
0.8	0.0	0.3307	-0.089	0.3395	-0.068	0.3284	-0.059	0.3378	-0.046	0.3273	-0.044	0.3370	-0.034
1.0	0.0	0.3108	-0.349	0.3197	-0.328	0.3027	-0.230	0.3122	-0.217	0.2987	-0.172	0.3085	-0.162

**Table 3**

Lower and upper bounds for the pull-in parameters of a micro/nanocantilever subjected to a compressive axial load with  $k=1.2$ , for several values of the vdW and Casimir parameters  $\alpha_W$ ,  $\alpha_C$ , and geometric ratio  $d/w$ .

$k=1.2$		$d/w=0$				$d/w=1$				$d/w=2$			
$\alpha_W$	$\alpha_C$	$r_l$	$\beta_l$	$r_u$	$\beta_u$	$r_l$	$\beta_l$	$r_u$	$\beta_u$	$r_l$	$\beta_l$	$r_u$	$\beta_u$
0.0	0.0	0.4476	0.7249	0.4556	0.7399	0.4918	0.5066	0.4999	0.5166	0.5185	0.3922	0.5267	0.3998
0.0	0.2	0.3350	0.3342	0.3427	0.3485	0.3458	0.2233	0.3538	0.2327	0.3512	0.1679	0.3593	0.1749
0.0	0.4	0.2741	0.0079	0.2819	0.0217	0.2743	0.0052	0.2825	0.0142	0.2744	0.0038	0.2827	0.0106
0.0	0.6	0.2296	-0.287	0.2374	-0.274	0.2230	-0.185	0.2312	-0.176	0.2199	-0.136	0.2283	-0.130
0.0	0.8	0.1937	-0.561	0.2016	-0.549	0.1819	-0.359	0.1902	-0.350	0.1764	-0.262	0.1849	-0.257
0.0	1.0	0.1633	-0.821	0.1712	-0.809	0.1472	-0.518	0.1555	-0.511	0.1397	-0.378	0.1483	-0.373
0.0	0.0	0.4476	0.7249	0.4556	0.7399	0.4918	0.5066	0.4999	0.5166	0.5185	0.3922	0.5267	0.3998
0.2	0.0	0.3967	0.4349	0.4048	0.4499	0.4165	0.2971	0.4249	0.3071	0.4271	0.2263	0.4357	0.2338
0.4	0.0	0.3586	0.1597	0.3668	0.1746	0.3647	0.1074	0.3734	0.1174	0.3679	0.0810	0.3768	0.0885
0.6	0.0	0.3273	-0.105	0.3356	-0.091	0.3236	-0.070	0.3325	-0.060	0.3218	-0.052	0.3310	-0.045
0.8	0.0	0.3004	-0.363	0.3088	-0.348	0.2889	-0.239	0.2980	-0.229	0.2833	-0.178	0.2927	-0.170
1.0	0.0	0.2766	-0.613	0.2850	-0.599	0.2585	-0.400	0.2677	-0.391	0.2499	-0.297	0.2594	-0.290

185 **5. Results**

186 The lower and upper bounds predicted by the present analytical approach for the normalized pull-in voltage  $\beta_l$  and  
 187  $\beta_u$  and for the normalized pull-in deflection  $r_u$  and  $r_l$  have been reported in Tables 1–3 for some particular set of the  
 188 parameters  $d/w$ ,  $\alpha_W$  and  $\alpha_C$  and for specific values of the axial load parameter  $k$  defined in (5) ranging between 0 and 1.5.  
 189 It can be observed that the results for vanishing compressive axial load, namely for  $k=0$ , recover those found in [21], thus  
 190 validating the present approach. Moreover, if the surface intermolecular parameters are greater than their critical values

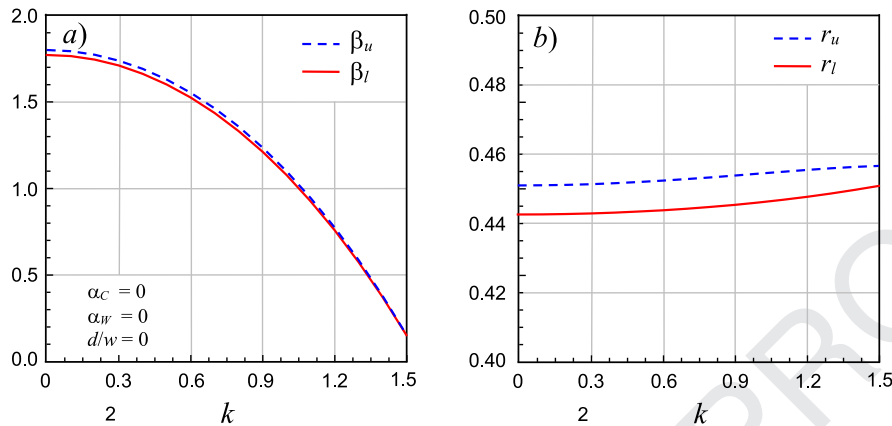


**Fig. 2.** Variations of lower and upper bounds for the pull-in voltage  $\beta_l$  and  $\beta_u$  (a) and tip deflection  $r_l$  and  $r_u$  (b) with the axial load parameter  $k$  for a microcantilever, for negligible fringing fields and intermolecular surface forces.

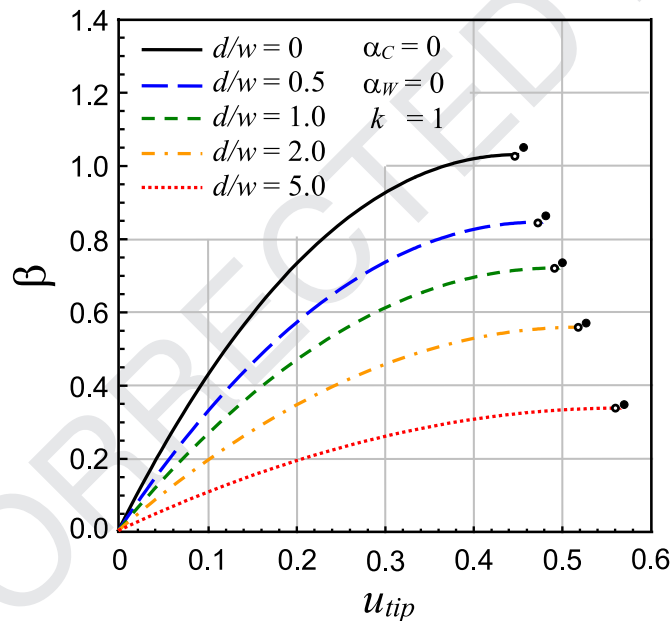


**Fig. 3.** Numerical results for the tip displacement  $u_{tip}$  as a function of the electrostatic loading parameters  $\beta$  provided by the shooting method, for  $k=1$  and for some values of the geometric ratio  $d/w$ . The lower and upper bounds of the pull-in parameters provided by the present analytical approach are denoted by small circles and small points, respectively.

191 that cause pull-in instability in the absence of electrostatic actuation and axial load, then a repulsive electrostatic force  
 192 characterized by negative values of  $\beta$  is required to prevent pull-in instability and the occurring of stiction. The results  
 193 obtained for  $\alpha_W = \alpha_C = 0$ , namely by neglecting the contribution of Casimir or vdW attractions, are significant for MEMS,  
 194 which are not affected by these forces.

195 The effects of the axial load parameter  $k$  on the lower and upper bounds for the pull-in parameters  $\beta_{pl}$  and  $r_{pl}$  are shown  
 196 in Fig. 2 for vanishing small fringing and intermolecular surface forces ( $d/w = \alpha_C = \alpha_W = 0$ ). These results clearly display that  
 197 the lower and upper analytical bounds are very close each other for  $k$  ranging between 0 and  $\pi/2$ , and thus they provide  
 198 very accurate estimates of the actual pull-in parameters  $\beta_{pl}$  and  $r_{pl}$ . Moreover, the pull-in voltage becomes null as the axial  
 199 load parameter tends to its limit value  $k = \pi/2$ , corresponding to the classical elastic buckling load of a EB cantilever beam.

200 The analytical bounds have been validated by comparison with the numerical solution of the nonlinear BVP (1) and (4)  
 201 calculated by using the command NDSolve of the *Mathematica* software (version number 8), which exploits the shooting  
 202 method for the numerical integration of two point BVP [36]. The variation of the tip deflection of the nanocantilever  $r = u(1)$   
 203 with the electrostatic loading parameter  $\beta$  obtained from the *Mathematica* software are reported in Fig. 3 for the same value  
 204 of the axial load parameter,  $k = 1$ , and for different values of the geometric ratio  $d/w$ . The largest pull-in voltage is attained  
 205 for  $d/w = 0$ , namely for a vanishing small fringing field occurring when the separation distance  $d$  is much smaller than the  
 206 beam width  $w$ . If the effects of fringing fields become more relevant, as it occurs for large values of the ratio  $d/w$ , then the  
 207 pull-in voltage  $\beta_{pl}$  decreases, whereas the pull-in tip deflection  $r_{pl}$  increases. In the following figures, we denote with small

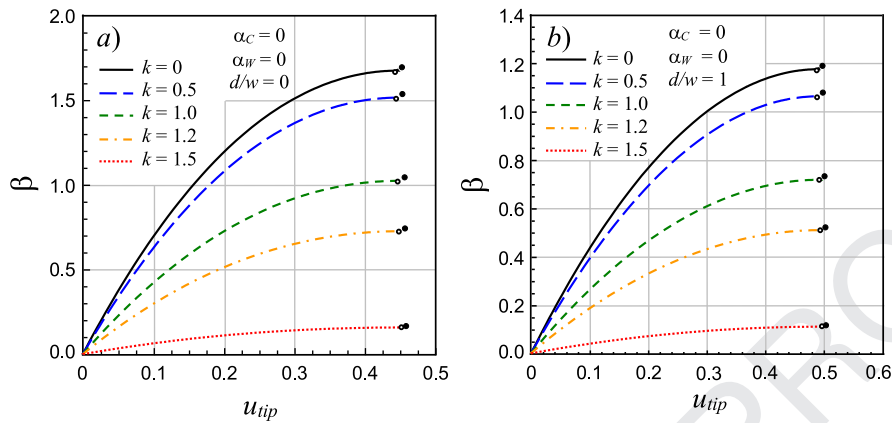


Fig. 4. Numerical results for the tip displacement  $u_{tip}$  as a function of the electrostatic loading parameters  $\beta$  provided by the shooting method, for some values  $k$  ranging between 0 and 1.5, for negligible intermolecular forces ( $\alpha_w = \alpha_c = 0$ ) and for geometric ratios  $d/w = 0$  (a) and  $d/w = 1$  (b). The lower and upper bounds of the pull-in parameters provided by the present analytical approach are denoted by small circles and small points, respectively.

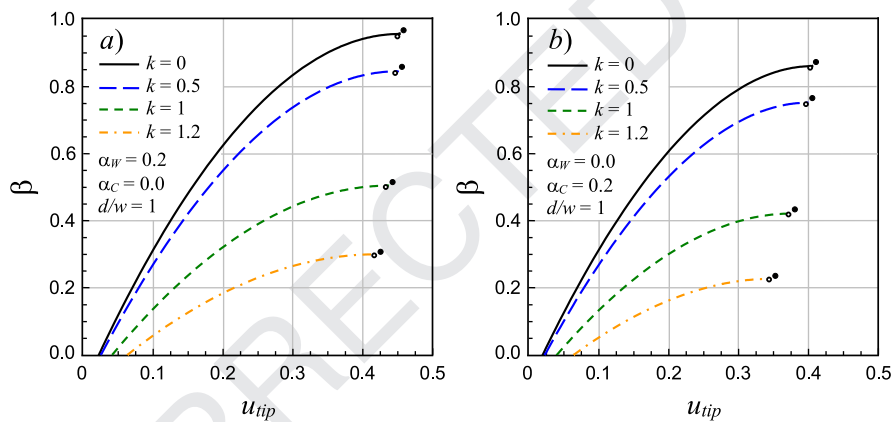


Fig. 5. Numerical results for the tip displacement  $u_{tip}$  as a function of the electrostatic loading parameters  $\beta$  provided by the shooting method, for some values  $k$  ranging between 0 and 1.5, for the geometric ratios  $d/w = 1$ , for vdW parameters  $\alpha_w = 0.2$  (a) and for Casimir parameters  $\alpha_c = 0.2$  (b). The lower and upper bounds of the pull-in parameters provided by the present analytical approach are denoted by small circles and small points, respectively.

208 circles and small points the lower and upper bounds for the pull-in parameters, respectively. It can be observed that the  
 209 exact pull-in parameters, namely the maximum point attained by the numerical curves plotted in Fig. 3, fall between the  
 210 lower and upper bounds.

211 The variations of the deflection  $r$  of the cantilever tip with the electrostatic loading parameter  $\beta$  obtained from the  
 212 *Mathematica* software are plotted in Figs. 4 and 5 for some specific set of the parameters  $d/w$ ,  $\alpha_w$  and  $\alpha_c$  and for a range  
 213 of values of the axial load parameter  $k$  between 0 and 1.5. These results show that the combined effects of fringing effect,  
 214 intermolecular surface forces and compressive axial load significantly reduce the pull-in voltage. In Fig. 4, no noticeable  
 215 effect of the axial load can be detected on the pull-in deflection, which is almost independent of  $k$  in the absence of inter-  
 216 molecular surface forces. A moderate reduction for the pull-in deflection as the axial load parameter  $k$  is increased is instead  
 217 observed in Fig. 5, due to the combined effects of the axial load and intermolecular forces. Note that the lower bounds for  
 218  $\beta$  and  $r$  almost coincide with the exact pull-in parameters predicted by numerical investigation. Moreover, Fig. 5 shows that  
 219 the intermolecular surface forces cause a deflection of the nanocantilever also in the absence of electric voltage, namely for  
 220  $\beta = 0$ .

221 The variations of the upper and lower bounds  $\beta_u$  and  $\beta_l$  with  $\alpha_w$  and  $\alpha_c$  are plotted in Fig. 6 for the range of values  
 222 of the axial load parameter  $k$ . This plot shows that the compressive axial load and the intermolecular surface forces have  
 223 similar effects on the electrostatic pull-in parameter, consisting in a significant reduction of the pull-in voltage. It can be  
 224 observed that the analytical estimates are very close and thus accurate for the full ranges of variation of the axial load  
 225 parameter and intermolecular surface forces.

226 The variations of the tip displacement  $u_{tip}$  with the vdW and Casimir parameters,  $\alpha_w$  and  $\alpha_c$ , provided by the numerical  
 227 integration procedure implemented in the *Mathematica* software are presented in Figs. 7a,b for vanishing electric actuation  
 228 ( $\beta = 0$ ) and for several values of the axial load parameter  $k$ . These plots reveal that pull-in instability may occur even in  
 229 the absence of electric voltage if the vdW or Casimir parameters exceed their maximum value  $\alpha_{w0}$  or  $\alpha_{c0}$ . Moreover they  
 230 show that an increase in the compressive axial load reduces the limit values of the intermolecular surface forces, but has

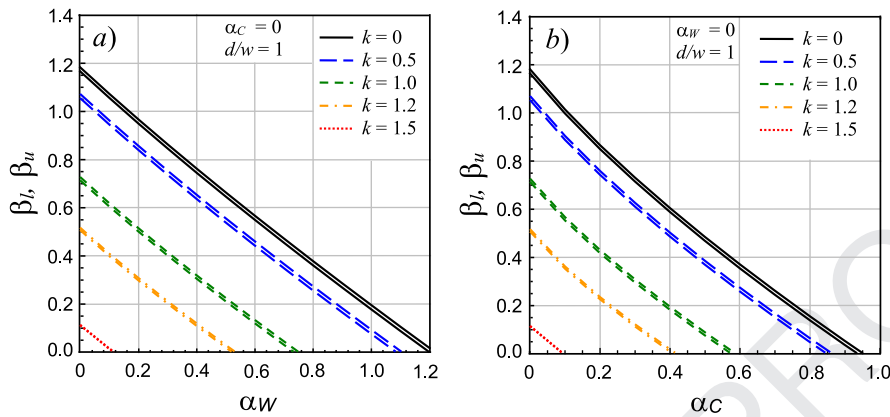


Fig. 6. Effects of vdW (a) and Casimir (b) attractions on the lower and upper analytical bounds for the pull-in voltage, for a range of values of  $k$  between 0 and 1.5.

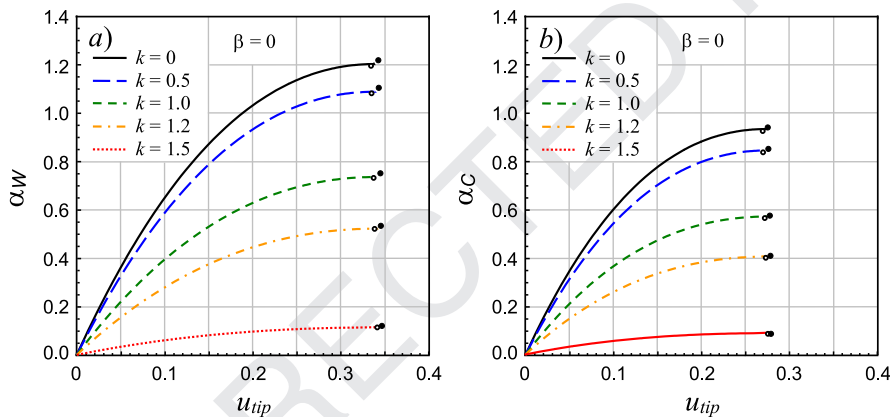


Fig. 7. Numerical results for the tip displacement  $u_{tip}$  as a function of the vdW (a) and Casimir (b) parameters  $\alpha_W$  and  $\alpha_C$  in the absence of electrostatic actuation ( $\beta = 0$ ) provided by the shooting method for some values  $k$  ranging between 0 and 1.5. The lower and upper bounds of the critical vdW and Casimir parameters provided by the analytical approach are denoted by small circles and small points, respectively.

**Table 4**  
Lower and upper bounds for the critical vdW and Casimir parameters  $\alpha_W$ ,  $\alpha_C$ , and corresponding critical tip deflections  $r_W$  and  $r_C$ .

$k$	$\alpha_{Wl}$	$r_{Wl}$	$\alpha_{Wu}$	$r_{Wu}$	$\alpha_{Cl}$	$r_{Cl}$	$\alpha_{Cu}$	$r_{Cu}$
0.0	1.1967	0.3350	1.2171	0.3423	0.9326	0.2694	0.9492	0.2756
0.5	1.0828	0.3357	1.1030	0.3430	0.8439	0.2700	0.8602	0.2762
1.0	0.7323	0.3379	0.7480	0.3449	0.5708	0.2717	0.5834	0.2777
1.2	0.5197	0.3392	0.5310	0.3458	0.4051	0.2728	0.4141	0.2784
1.5	0.1129	0.3418	0.1151	0.3466	0.0881	0.2750	0.0898	0.2790

no significant influence on the pull-in deflection. In these plots, the lower and upper bounds for the parameter  $\alpha_{W0}$  and  $\alpha_{C0}$  causing the pull-in of the device and the corresponding pull-in deflection  $r_{W0}$  and  $r_{C0}$  are denoted by small circles and points. The analytical predictions for the lower and upper bounds agree very well with the numerical results obtained by the *Mathematica* software.

Since the Casimir force is effective at larger distances than the vdW force, then pull-in instability caused by the effect of the Casimir force is found to occur at smaller tip deflections, and thus at larger separation distances between the electrodes, than the pull-in tip instability caused by the action of the vdW force. The lower and upper bounds for the critical vdW and Casimir parameters  $\alpha_{W0}$  and  $\alpha_{C0}$  for a compressed nanocantilever in the absence of electrostatic actuation can be found also in Table 4 for the considered range of values of the axial load parameter  $k$ .

**6. Conclusions**

A useful analytical method for accurately predicting the pull-in instability of a micro- or nanocantilever subjected to electrostatic actuation, compressive axial load and vdW or Casimir attractions has been proposed as an alternative to the numerical solution of the extremely nonlinear BVP. After the influence of the compressive axial load on the pull-in

instability has been examined, the accuracy of the analytical lower and upper bounds has been verified by comparison with the numerical solution of the nonlinear BVP obtained by using the shooting method procedure available in the *Mathematica* package. In particular, the lower bounds are found to be very close to the exact pull-in parameters.

The provided estimates make the present study particularly significant for developing new practical applications in the field of MEMS and NEMS and make it crucial for the validation of many numerical investigations. We indeed recover that the interaction between the compressive axial load, intermolecular surface forces and fringing field can significantly reduce the pull-in voltage [10–12]. If the contribution of the compressive axial load is neglected then the pull-in voltage may be considerably overestimated and this inaccuracy may lead to unexpected damage during device operation. Therefore, the present investigation may be very helpful for assuring the safe operation of MEMS and NEMS current devices, since it allows avoiding any potential breakage by predicting accurate bounds for the critical pull-in characteristics.

## Acknowledgment

Support from the Italian "Gruppo Nazionale di Fisica Matematica" INdAM-GNFM is gratefully acknowledged.

## References

- [1] O.Y. Loh, H.D. Espinosa, Nanoelectromechanical contact switches, *Nat. Nanotech.* 7 (2012) 283–295.
- [2] A.M. Ionescu, Nano-electro-mechanical (NEM) memory devices, in: A.N. Chen, J. Hutchby, V. Zhirnov, G. Bourianoff (Eds.), *Emerging Nanoelectronic Devices*, John Wiley & Sons Ltd., 2014, pp. 123–136.
- [3] A. Ramezani, A. Alasty, J. Akbari, Closed-form solutions of the pull-in instability in nano-cantilevers under electrostatic and intermolecular surface forces, *Int. J. Solids Struct.* 44 (2007) 4925–4941.
- [4] W.H. Lin, Y.P. Zhao, Pull-in instability of micro-switch actuators, model review, *Int. J. Nonlin. Sci. Numer. Simul.* 9 (2008) 175–183.
- [5] W.C. Chuang, H.L. Lee, P.Z. Chang, Y.C. Hu, Review on the modeling of electrostatic MEMS, *Sensors* 10 (2010) 6149–6171.
- [6] W.M. Zhang, H. Yan, Z.K. Peng, G. Meng, Electrostatic pull-in instability in MEMS/NEMS. A review, *Sens. Actuators A Phys* 214 (2014) 187–218.
- [7] S.P. Timoshenko, J.M. Gere, *Theory of Elastic Stability*, second ed., Dover, New York, 2009.
- [8] D. Elata, S. Abu-Salih, Analysis of a novel method for measuring residual stress in micro-systems, *J. Micromech. Microeng.* 15 (2005) 921.
- [9] S. Abu-Salih, D. Elata, Experimental validation of electromechanical buckling, *J. Microelectro-mech. Syst.* 15 (2006) 1656–1662.
- [10] S.A. Emam, A general nonlocal nonlinear model for buckling of nanobeams, *Appl. Math. Model* 37 (2013) 6929–6939.
- [11] M.A. Eltaher, M.E. Khater, S.A. Emam, A review on nonlocal elastic models for bending, buckling, vibrations, and wave propagation of nanoscale beams, *Appl. Math. Model* 40 (2016) 4109–4128.
- [12] M. Shaat, A. Abdelkefi, Buckling characteristics of nanocrystalline nano-beams, *Int. J. Mech. Mater. Des.* (2017) 1–19, doi:10.1007/s10999-016-9361-2.
- [13] E. Buks, M.L. Roukes, Stiction, adhesion energy, and the Casimir effect in micromechanical systems, *Phys. Rev. B* 63 (2001) 033402.
- [14] S. Basu, A. Prabhakar, E. Bhattacharya, Estimation of stiction force from electrical and optical measurements on cantilever beams, *J. Microelectromech. Syst.* 16 (2007) 1254–1262.
- [15] T.J. Wagner, D. Vella, Switch on, switch off: stiction in nanoelectromechanical switches, *Nanotech* 24 (2013) 275501.
- [16] E.M. Abdel-Rahman, M.I. Younis, A.H. Nayfeh, Characterization of the mechanical behavior of an electrically actuated microbeam, *J. Micromech. Microeng.* 12 (2002) 759–766.
- [17] L.X. Zhang, Y.P. Zhao, Electromechanical model of RF MEMS switches, *Microsys. Tech.* 9 (2003) 420–426.
- [18] Y. Zhang, Y.P. Zhao, Numerical and analytical study on the pull-in instability of micro-structure under electrostatic loading, *Sens. Actuators A Phys.* 127 (2006) 366–380.
- [19] C.W. Lim, C. Li, J.-L. Yu, The effects of stiffness strengthening nonlocal stress and axial tension on free vibration of cantilever nanobeams, *Interact. Multiscale Mech.* 2 (2009) 223–233.
- [20] Y.Y. Zhang, C.M. Wang, N. Challamel, Bending, buckling and vibration of hybrid nonlocal beams, *J. Eng. Mech. ASCE* 136 (2010) 562–574.
- [21] E. Radi, G. Bianchi, L. di Ruvo, Upper and lower bounds for the pull-in parameters of a micro- or nanocantilever on a flexible support, *Int. J. Nonlin. Mech.* 92 (2017) 176–186.
- [22] R. Soroush, A. Koochi, A.S. Kazemi, A. Noghrehabadi, H. Haddadpour, M. Abadyan, Investigating the effect of Casimir and van der Waals attractions on the electrostatic pull-in instability of nano-actuators, *Phys. Scr.* 82 (2010) 045801.
- [23] A.C. Eringen, *Nonlocal Continuum Field Theories*, Springer, 2002.
- [24] H.S. Park, Surface stress effects on the critical buckling strains of silicon nanowires, *Comput. Mater. Sci.* 51 (2012) 396–401.
- [25] S. Cuenot, C. Frétygn, S. Demoustier-Champagne, B. Nysten, Surface tension effect on the mechanical properties of nanomaterials measured by atomic force microscopy, *Phys. Rev. B* 69 (2004) 165410.
- [26] G.-F. Wang, X.-Q. Feng, Surface effects on buckling of nanowires under uniaxial compression, *Appl. Phys. Lett.* 94 (2009) 141913.
- [27] N. Challamel, I. Elishakoff, Surface stress effects may induce softening: Euler-Bernoulli and Timoshenko buckling solutions, *Phys. E Low Dimens. Syst. Nanostruct.* 44 (2012) 1862–1867.
- [28] A. Farrokhabadi, A. Mohebbshahedin, R. Rach, J.S. Duan, An improved model for the cantilever NEMS actuator including the surface energy, fringing field and Casimir effects, *Phys. E Low Dimens. Syst. Nanostruct.* 75 (2016) 202–209.
- [29] Y.T. Beni, A. Koochi, M. Abadyan, Theoretical study of the effect of Casimir force, elastic boundary conditions and size dependency on the pull-in instability of beam-type NEMS, *Phys. E Lowdim. Sys. Nanostruct.* 43 (2011) 979–988.
- [30] W.D. Yang, X. Wang, C.Q. Fang, G. Lu, Electromechanical coupling characteristics of carbon nanotube reinforced cantilever nano-actuator, *Sens. Actuators A Phys.* 220 (2014) 178–187.
- [31] A. Koochi, A. Kazemi, F. Khandani, M. Abadyan, Influence of surface effects on size-dependent instability of nano-actuators in the presence of quantum vacuum fluctuations, *Phys. Scripta* 85 (2012) 035804.
- [32] A.W. McFarland, M.A. Poggi, M.J. Doyle, L.A. Bottomley, J.S. Colton, Influence of surface stress on the resonance behavior of microcantilevers, *Appl. Phys. Lett.* 87 (2005) 053505.
- [33] A. Ramezani, A. Alasty, J. Akbari, Influence of van der Waals force on the pull-in parameters of cantilever type nanoscale electrostatic actuators, *J. Microsyst. Technol.* 12 (2006) 1153–1161.
- [34] J. Duan, Z. Li, J. Liu, Pull-in instability analyses for NEMS actuators with quartic shape approximation, *Appl. Math. Mech.* 37 (2016) 303–314.
- [35] B. Yang, Positive solution for a fourth order boundary value problem, *Electron. J. Qual. Theory Differ. Equ.* 3 (2005) 1–17.
- [36] S. Wolfram, *The Mathematica Book*, Cambridge University Press, 1996.